 Related Commentary, page 4341

Endothelial epsin deficiency decreases tumor growth by enhancing VEGF signaling

Satish Pasula,[1] Xiaofeng Cai,[1] Yunzhou Dong,[1] Mirko Messa,[2] John McManus,[1] Baojun Chang,[1] Xiaolei Liu,[1] Hua Zhu,[1] Robert Silasi Mansat,[1] Seon-Joo Yoon,[1] Scott Hahn,[1] Jacob Keeling,[1] Debra Saunders,[1] Genevieve Ko,[2] John Knight,[1] Gail Newton,[3] Francis Luscinskas,[3] Xiaohong Sun,[1] Rheal Towner,[1] Florea Lupu,[1] Lijun Xia,[1,4] Ottavio Cremona,[5,6,7] Pietro De Camilli,[2] Wang Min,[8] and Hong Chen[1,4]

[1]Cardiovascular Biology Program, Oklahoma Medical Research Foundation, Oklahoma City, Oklahoma, USA. [2]Howard Hughes Medical Institute, Department of Cell Biology, and Program in Cellular Neuroscience, Neurodegeneration and Repair, Yale University School of Medicine, New Haven, Connecticut, USA. [3]Center for Excellence in Vascular Biology, Department of Pathology, Brigham and Women's Hospital, Harvard University, Boston, Massachusetts, USA. [4]Department of Biochemistry and Molecular Biology, University of Oklahoma Health Science Center, Oklahoma City, Oklahoma, USA. [5]IFOM, the FIRC Institute of Molecular Oncology Foundation, [6]Università Vita—Salute San Raffaele, and [7]Istituto Nazionale di Neuroscienze, Milano, Italy. [8]Department of Pathology, Interdepartmental Program in Vascular Biology and Therapeutics, Yale University School of Medicine, New Haven, Connecticut, USA.

Epsins are a family of ubiquitin-binding, endocytic clathrin adaptors. Mice lacking both epsins 1 and 2 (*Epn1/2*) die at embryonic day 10 and exhibit an abnormal vascular phenotype. To examine the angiogenic role of endothelial epsins, we generated mice with constitutive or inducible deletion of *Epn1/2* in vascular endothelium. These mice exhibited no abnormal phenotypes under normal conditions, suggesting that lack of endothelial epsins 1 and 2 did not affect normal blood vessels. In tumors, however, loss of epsins 1 and 2 resulted in disorganized vasculature, significantly increased vascular permeability, and markedly retarded tumor growth. Mechanistically, we show that VEGF promoted binding of epsin to ubiquitinated VEGFR2. Loss of epsins 1 and 2 specifically impaired endocytosis and degradation of VEGFR2, which resulted in excessive VEGF signaling that compromised tumor vascular function by exacerbating nonproductive leaky angiogenesis. This suggests that tumor vasculature requires a balance in VEGF signaling to provide sufficient productive angiogenesis for tumor development and that endothelial epsins 1 and 2 negatively regulate the output of VEGF signaling. Promotion of excessive VEGF signaling within tumors via a block of epsin 1 and 2 function may represent a strategy to prevent normal angiogenesis in cancer patients who are resistant to anti-VEGF therapies.

Introduction

Angiogenesis, the formation of new blood vessels from preexisting vessels, is essential for embryogenesis and postnatal organ repair under physiological conditions. However, under pathological conditions, such as in cancer, angiogenesis is also crucial for tumor cells to obtain oxygen and nutrients to sustain aggressive growth. VEGF signaling plays a central role in physiological and pathological angiogenesis, such as that occurring in ischemia, diabetes, and cancer (1). VEGF binds to its receptor VEGFR2 (also known as Flk-1 or KDR) on ECs, inducing dimerization and autophosphorylation to initiate signaling cascades required for EC migration and proliferation (2). Increased VEGF signaling causes tortuous vasculature and vascular leakage in tumors.

The epsins are a family of ubiquitin-binding endocytic clathrin adaptor proteins (3–7). Mammals express 3 epsins, which are encoded by 3 different genes (*Epn1*, *Epn2*, and *Epn3*) (8). Epsins 1 and 2 are broadly expressed in all tissues (3, 4, 9), while epsin 3 is heterogeneously expressed, with high levels of expression only in the stomach (8). Mice lacking either epsin 1 or 2 exhibit no abnormal phenotype, indicating redundant functions. However, epsins 1 and 2 double-KO (DKO) mice die at E10 (9). Although an abnormal vascular phenotype is prominent in DKO embryos, it is unclear by which mechanism and in which cell type epsins 1 and 2 are required for angiogenesis. In addition, whether epsin-regulated angiogenesis is important in adult animals remains to be addressed.

We generated mouse models with constitutive or inducible deletion of epsins 1 and 2 specifically in ECs. These mice showed no obvious phenotypic defects under normal conditions. However, adult mice lacking endothelial epsins 1 and 2 exhibited highly disorganized vascular structures and markedly increased vascular permeability in tumors due to heightened VEGF/VEGFR2 signaling, which increased nonproductive tumor angiogenesis and retarded tumor growth. VEGF promotes epsin binding to ubiquitinated VEGFR2, and this interaction is required for endocytosis and degradation of VEGFR2. Our results indicate that epsins 1 and 2 function as unique attenuators of VEGF signaling, that their absence produces excessive leaky tumor angiogenesis, and that targeting epsin function may represent a potential antitumor strategy by promoting nonproductive tumor angiogenesis.

Results

Loss of endothelial epsins 1 and 2 results in decreased tumor growth. To investigate the role of endothelial epsins 1 and 2 in the adult vascular system, we generated mouse models that selectively lack epsins 1 and 2 in ECs. We first created mice with a conditional epsin 1 allele (*Epn1*$^{fl/fl}$) (Supplemental Figure 1A; supplemental material available online with this article; doi:10.1172/JCI64537DS1)

Authorship note: Satish Pasula, Xiaofeng Cai, and Yunzhou Dong contributed equally to this work.

Conflict of interest: The authors have declared that no conflict of interest exists.

Citation for this article: *J Clin Invest.* 2012;122(12):4424–4438. doi:10.1172/JCI64537.

and crossed them with epsin 2–KO mice (*Epn2*$^{-/-}$) (9) to obtain *Epn1*$^{fl/fl}$*Epn2*$^{-/-}$ mice. These were further crossed with mice expressing tamoxifen-inducible Cre recombinase under control of the VE-cadherin promoter (*VEcad-ER*^{T2}) (refs. 10, 11, and Supplemental Figure 1B). To produce EC-specific DKO mice (EC-iDKO) (Supplemental Figure 1, B and D), 10-week-old sex- and genetic background–matched WT or *Epn1*$^{fl/fl}$*Epn2*$^{-/-}$*VEcad-ER*^{T2} mice were injected i.p. with 5 mg/kg (body weight) of 4-hydroxytamoxifen (10 mg/ml of 4-hydroxytamoxifen in 20% ethanol/80% DMSO) per day for 5–7 consecutive days to obtain WT or EC-iDKO. Deletion of epsin 1 was validated by Western blot analysis of ECs isolated from EC-iDKO (Supplemental Figure 1E). Although global deletion of epsins 1 and 2 results in embryonic lethality and prominent vascular defects (9), EC-iDKO mice survive indistinguishably from WT, displaying no obvious abnormalities. To rule out any undesirable effects tamoxifen-activated Cre may produce, we crossed WT or *Epn1*$^{fl/fl}$*Epn2*$^{-/-}$ mice with mice constitutively expressing Cre recombinase under control of the VE-cadherin promoter (*VEcad-Cre*) (12) to obtain *WT/VEcad-Cre* or *Epn1*$^{fl/fl}$*Epn2*$^{-/-}$*VEcad-Cre* mice, respectively. Deletion of epsin 1 was observed by Western blot analysis only in ECs of *Epn1*$^{fl/fl}$*Epn2*$^{-/-}$*VEcad-Cre* mice. These mice were designated EC-DKO (Supplemental Figure 1F). *VEcad-Cre* is known to be active as early as E7.5, with progressive activation from E8.5–E13.5. Although epsins 1 and 2 are important for embryonic angiogenesis, lack of full penetrance of *VEcad-Cre* until later stages of embryonic development may alleviate the embryonic vascular phenotype and contribute to survival of EC-DKO mice to adulthood. We did not observe any significant vascular abnormalities in these adult animals under normal physiological conditions. We then sought to determine whether endothelial epsins 1 and 2 are important under pathological conditions such as tumor angiogenesis (13).

To test this, we subcutaneously implanted mouse Lewis lung carcinoma (LLC) cells and melanoma cells (mouse skin cancer cell line B16F10) into WT or EC-iDKO mice at 1 week after the final 4-hydroxytamoxifen injection. Strikingly, in both LLC- and melanoma-implanted mice, we observed fewer tumors, with over 50% reduction of tumor incidence in EC-iDKO mice compared with WT mice (Figure 1, A and B). Moreover, tumors in EC-iDKO mice had a much slower growth rate (Figure 1, A and B) and markedly reduced sizes (Supplemental Figure 2, A and B). Likewise, EC-DKO mice implanted with LLC tumor cells exhibited reduced tumor incidence and attenuated tumor growth compared with WT (Supplemental Figure 2C), suggesting that endothelial epsins 1 and 2 play a critical role in promoting tumor development and progression. These promising results prompted us to examine additional tumor types. We tested the role of endothelial epsins 1 and 2 in development of an orthotopic glioma tumor. GL261 glioma cells derived from an aggressive mouse glioblastoma that closely mimics its human counterpart in its invasive and angiogenic properties (14) were orthotopically implanted in the right forebrain of WT and EC-iDKO mice. MRI imaging analysis 24 days after tumor inoculation revealed that tumors in EC-iDKO mice were significantly smaller than those of WT (Figure 1C and Supplemental Figure 2D). Accordingly, glioma-bearing EC-iDKO outsurvived WT with glioma for an average of 11 days, which corresponds to a survival time of approximately 1 year in human patients (Figure 1D). Remarkably, 20% of EC-iDKO tumor-bearing mice became tumor free and survived similarly to normal mice (Figure 1D).

To assess the role of endothelial epsins 1 and 2 in spontaneous tumor growth, we established 2 spontaneous tumor models in WT or EC-iDKO mice. In the azoxymethane/dextran sodium sulphate (AOM/DSS) induced colorectal tumor model, WT and EC-iDKO were given a single dose of AOM via i.p. injection 1 week after 4-hydroxytamoxifen administration. One week later, the mice were given DSS in drinking water for 7 days. Following DSS treatment, WT and EC-iDKO mice were euthanized every week from 16–20 weeks. The colorectal region was longitudinally dissected and examined for tumors. We observed significantly reduced tumor incidence and decreased tumor growth in EC-iDKO mice compared with WT (Figure 1E and Supplemental Figure 2E). To corroborate the role of endothelial epsins 1 and 2 in controlling colorectal tumor growth we used another spontaneous tumor model, the Transgenic Adenocarcinoma of Mouse Prostate (TRAMP) cancer model. We generated our experimental animals by crossing EC-iDKO or WT mice with TRAMP mice to generate TRAMP-EC-iDKO or TRAMP-WT mice. Ten-week-old and genetic background–matched male TRAMP-EC-iDKO or TRAMP-WT mice were i.p. injected with 4-hydroxytamoxifen to induce deletion of endothelial epsin 1. Mortality was recorded, and survival rate was plotted for TRAMP mice with or without endothelial epsins 1 and 2. Mice were also sacrificed at weeks 20, 24, 28, 32, and 36 and examined for prostate tumors. We observed a significant decrease in the mortality rate of TRAMP-EC-iDKO compared with TRAMP-WT mice (Figure 1F). Moreover, only very small tumors were found in TRAMP-EC-iDKO mice at 36 weeks, a time at which most TRAMP-WT had developed large tumors in the prostate and nearby seminal vesicles (Supplemental Figure 2F). Collectively, our data suggest that endothelial epsins 1 and 2 are critical for tumor growth and function, which is achieved by modulating tumor angiogenesis in these mice.

Loss of endothelial epsins 1 and 2 caused disorganized and leaky tumor vessels and enhanced VEGFR2 signaling. To determine whether lack of endothelial epsins 1 and 2 reduces tumor growth by disrupting tumor angiogenesis, we examined tumor vasculatures in immunostained frozen sections. In EC-iDKO tumors, the blood vessel marker CD31 revealed enlarged vessels with an average diameter more than 2-fold larger than the average diameter in WT tumors (Figure 2, A and B). These vessels were also highly disorganized and tortuous (Figure 2, A and B). Enlarged EC-iDKO tumor vessels compared with WT tumor vessels showed negligible mural cell coverage, as revealed by coimmunostaining with CD31 and α-SMA, a mural cell marker (Supplemental Figure 3A), suggesting that these tumor vessels are more fragile and immature. To test whether the tumor vessels were functional, we i.v. injected 2×10^6 kDa lysine fixable FITC-dextran into WT or EC-iDKO mice displaying tumors. CD31 immunostaining revealed that, compared with WT, very few EC-iDKO tumor vessels contained FITC-dextran and the vessels exhibited extensive extravascular leakage of FITC-dextran (Figure 2B), suggesting that enlarged EC-iDKO tumor vessels were poorly perfused. This may lead to impaired oxygen and nutrient supply and thus decreased tumor growth in EC-iDKO mice.

Tumor vessels are known to have increased permeability induced by elevated VEGF signaling (1, 13, 15). The enlarged and hyperleaky tumor vessels in EC-iDKO mice may result from an inappropriately high level of VEGF signaling. We therefore asked whether this phenotype in EC-iDKO tumors was a result of increased VEGF expression, but this was ruled out because no significant difference in the expression of VEGF was found in WT compared

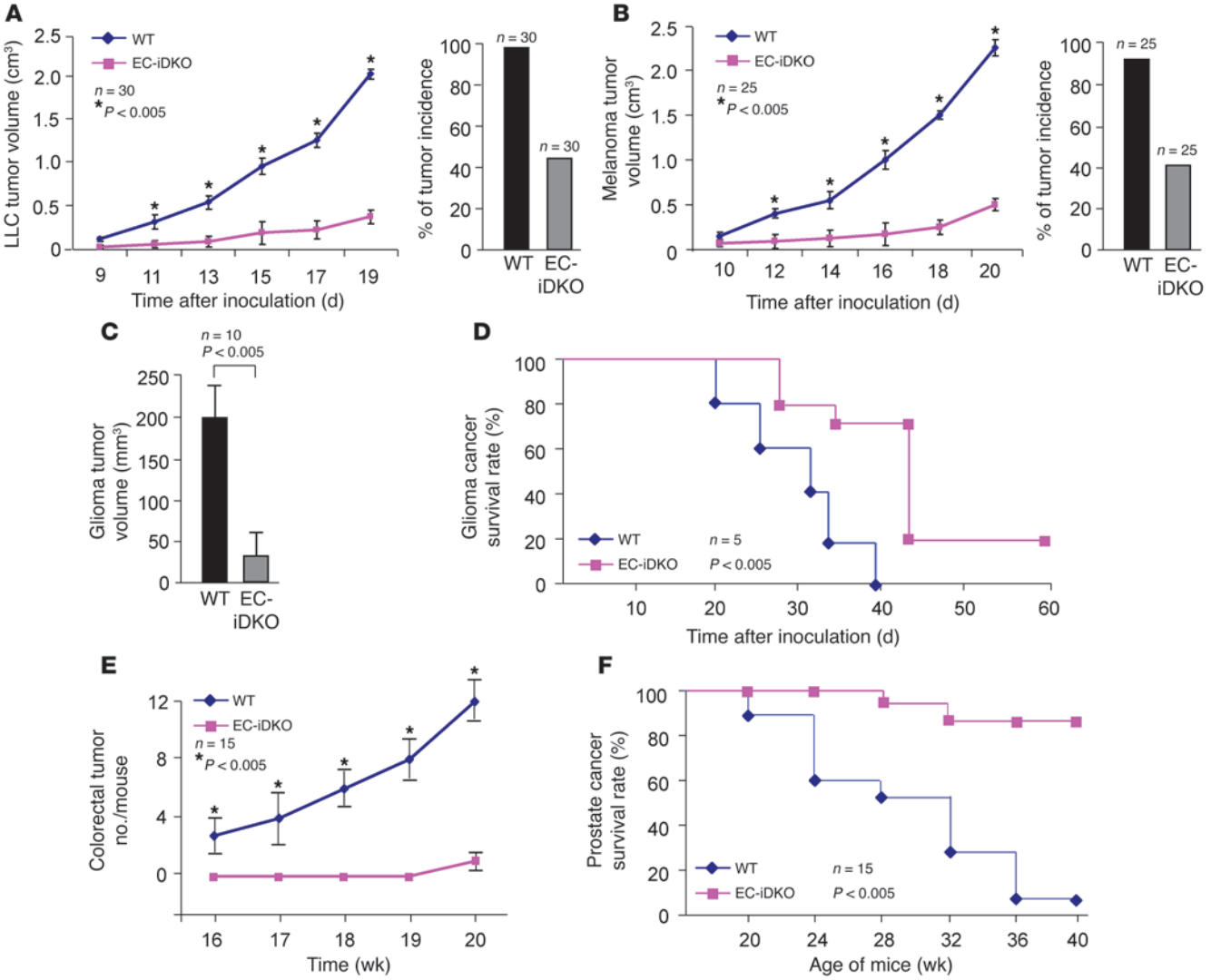

Figure 1

Loss of endothelial epsins 1 and 2 retards tumor growth. (**A**) LLC tumor size was measured every other day from day 9 through 19 after inoculation of LLC tumor cells into WT and EC-iDKO mice. LLC tumor incidence is shown on right. (**B**) Melanoma tumor size measured in WT and EC-iDKO from day 10 through 20 after inoculation of melanoma tumor cells. Melanoma tumor incidence is on right. (**C**) Average tumor volume of mouse brain *T2*-weighted MRI images for WT and EC-iDKO gliomas 24 days following GL261 cells injection. (**D**) Percentage of glioma cancer survival rate in WT and EC-iDKO mice. (**E**) The number of tumors observed in the colorectal region of WT and EC-iDKO mice euthanized after indicated number of weeks after AOM and DSS treatment. (**F**) Percentage of male TRAMP mice surviving in the presence or absence of endothelial epsins 1 and 2.

with EC-iDKO tumors (Supplemental Figure 3, B and C). We then investigated whether VEGFR2, the master receptor of VEGF, was elevated in tumors isolated from WT and EC-iDKO mice. The levels of total and phosphorylated VEGFR2 were increased strikingly in EC-iDKO tumors compared with WT tumors; however, no increases were detected for other receptors implicated in angiogenic pathways, including PDGFR-β, TGFβ-R1 and EGFR (Figure 2C), suggesting that loss of endothelial epsins 1 and 2 selectively affects VEGFR2 signaling. Furthermore, inhibiting VEGFR2 signaling by i.v. injecting a VEGFR2 kinase inhibitor reduced the size of LLC tumors in WT mice, but increased it in EC-iDKO mice (Supplemental Figure 4A). This "paradoxical" outcome prompted us to further examine the tumor vasculature and cancer cell apoptosis upon treatment with the inhibitor. The inhibitor markedly reduced VEGFR2 phosphorylation in HUVECs in response to VEGF (Supplemental Figure 4B). Interestingly, CD31 and TUNEL immunostaining of tumor samples revealed fewer tumor vessels (Supplemental Figure 4C) and more apoptotic tumor cells (Supplemental Figure 4D) in WT mice treated with the inhibitor. However, compared with control EC-iDKO mice, EC-iDKO mice treated with the inhibitor displayed less dilated and more "normal" appearing tumor vessels (Supplemental Figure 4C) and fewer apoptotic tumor cells (Supplemental Figure 4D), reflecting the fact that retarded tumor growth in the absence of endothelial epsins 1 and 2 is dependent upon VEGFR2 function.

VEGFR2 but not other angiogenic signaling is augmented in ECs lacking epsins 1 and 2. To further test the hypothesis that absence of endothelial epsins 1 and 2 specifically augments VEGFR2 signaling,

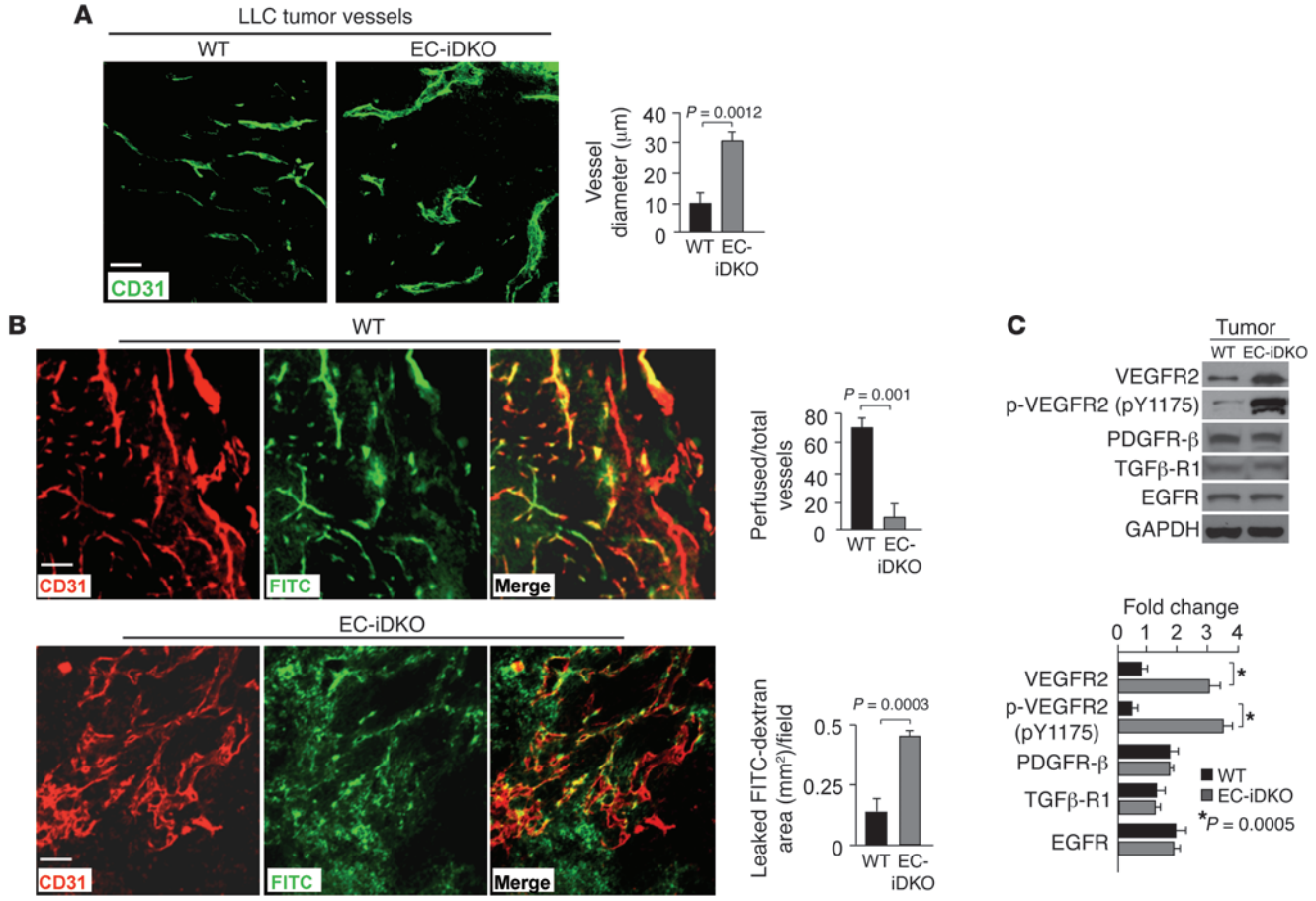

Figure 2

Enlarged leaky tumor vessels and elevated VEGFR2 signaling by loss of endothelial epsins 1 and 2. (**A**) LLC tumor vessels in WT and EC-iDKO mice revealed by CD31 immunostaining. Quantification of vessel diameter is on right. (**B**) LLC tumor vessels in WT and EC-iDKO mice after FITC-dextran perfusion observed by CD31 immunostaining. Quantification of perfused vessels and leaked FITC-dextran area is on right. (**C**) Western blotting analysis of indicated proteins in tumor tissue lysates from WT and EC-iDKO mice. Quantification of fold change normalized according to loading control GAPDH is on right. n = 10 (**A** and **B**); n = 5 (**C**). Scale bars: 50 μm (**A** and **B**).

we isolated primary ECs from WT or *Epn1*$^{fl/fl}$*Epn2*$^{-/-}$*VEcad-ER*^{T2} *Cre* mice and treated the cells with tamoxifen to ablate epsin 1 expression and obtain WT or DKO mouse ECs (MECs) (Figure 3A). To directly examine VEGF signaling, we stimulated WT or DKO MECs with 50 ng/ml VEGF for 0, 5, and 15 minutes. VEGF signaling was determined by phosphorylation of VEGFR2, PLC-γ, Akt, and ERK. We observed that VEGF signaling was dramatically increased in DKO MECs, reflected by elevated phosphorylation of VEGFR2, PLC-γ, Akt, and ERK (Figure 3, A and C). This increase in VEGF signaling could not be attributed to elevated VEGF production in DKO MECs because *VEGF* levels were not increased in these cells relative to WT MECs (Figure 3D). In parallel, using siRNA-mediated knockdown of epsins 1 and 2 in HUVECs, we observed augmented VEGFR2 signaling similar to that of DKO MECs after treatment with 50 ng/ml VEGF for 0, 5, 10, 15, and 30 minutes (Figure 3B). Moreover, prolonged VEGFR2 phosphorylation was apparent in epsin-deficient HUVECs compared with controls (Figure 3B). To determine whether other angiogenic signaling pathways are affected by loss of epsins 1 and 2, we examined FGF, PDGF, EGF, and TGF-β signaling pathways using siRNA-mediated knockdown of epsins 1 and 2 in HUVECs (Figure 3, E–H). VEGF signaling was again augmented (Figure 3, B and C, and Supplemental Figure 5, A–C), but there was no increase in signaling for FGF (Figure 3E and Supplemental Figure 5, A-C), PDGF (Figure 3F and Supplemental Figure 5C), EGF (Figure 3G and Supplemental Figure 5, B and C), or TGF-β (Figure 3H and Supplemental Figure 5D). Collectively, these data indicate that loss of endothelial epsins 1 and 2 elevates VEGFR2 signaling specifically.

To further assess whether loss of endothelial epsins 1 and 2 directly upregulates VEGFR2 signaling in vivo, we measured the permeability of blood vessels responding to VEGF in the absence of endothelial epsins 1 and 2 using Evans blue dye extravasation assay (16). WT or EC-iDKO mice were injected i.v. with 1% Evans blue dye and then injected intradermally with 10 μl VEGF (200 ng/μl) or PBS into the ear. VEGF-induced permeability of blood vessels was assessed by dye extravasation, which was quantified after extraction of the extravasated dye from the ears. As shown in Figure 3I, PBS produced little dye extravasation in either WT or EC-iDKO mice maintaining a quiescent vasculature, once again suggesting that endothelial epsins 1 and 2 are dispensable for maintenance of established vasculature in adults. How-

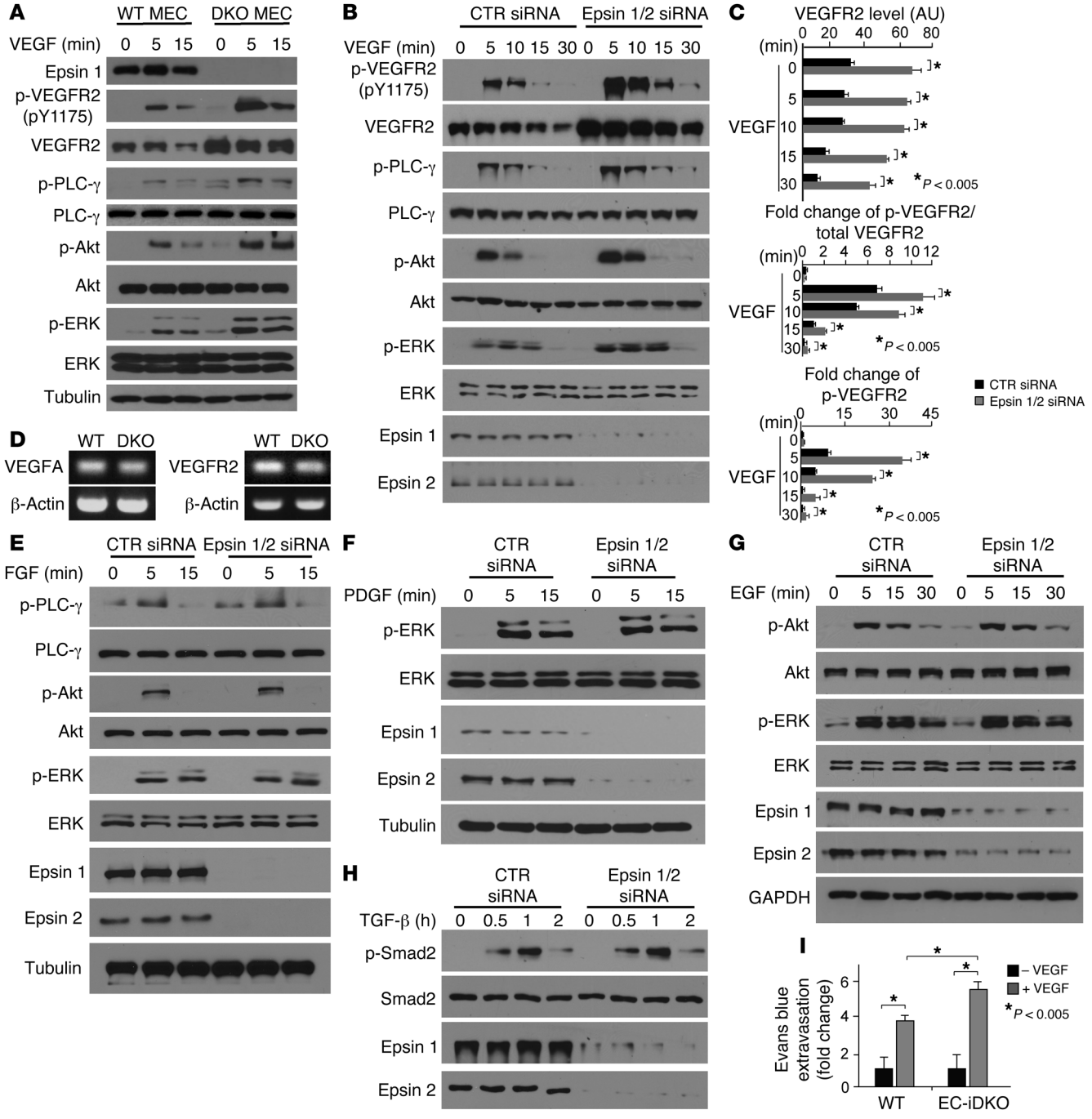

Figure 3

VEGF but not other angiogenic signaling is heightened in ECs lacking epsins 1 and 2. (**A** and **B**) WT or DKO MECs (**A**) or HUVECs transfected with either control siRNA or epsins 1 and 2 siRNAs (**B**) were stimulated with VEGF-A (50 ng/ml) and VEGF signaling was analyzed by Western blotting. (**C**) Quantification of total VEGFR2 and fold change of phospho-VEGFR2 to total VEGFR2 in HUVECs treated with either control or epsin 1 and 2 siRNAs. (**D**) RT-PCR showing *VEGF-A* and *VEGFR2* expression in WT and DKO MECs. (**E**–**H**) VEGF but not FGF, PDGF, EGF, or TGF-β signaling is augmented in the absence of epsins 1 and 2. HUVECs transfected with either control or epsins 1 and 2 siRNAs were stimulated with FGF (25 ng/ml) (**E**), PDGF (25 ng/ml) (**F**), EGF (30 ng/ml) (**G**), or TGF-β (5 ng/ml) (**H**) and analyzed by Western blotting. (**I**) VEGF-induced augmented ear vessel permeability revealed by Evans blue dye extravasation. $n > 5$ per group in all panels.

ever, VEGF induced significant dye extravasation in WT, mice and this vascular leakage was even more prominent in EC-iDKO mice, suggesting that the VEGF response is elevated in EC-iDKO relative to WT mice (Figure 3I).

Restoring Notch function does not rescue elevated VEGFR2 signaling caused by loss of endothelial epsins 1 and 2. In a previous study,we showed that epsins 1 and 2 are required for activation of the Notch pathway (9), which is important for embryonic vascular development

(17–19), consistent with studies in Drosophila (20, 21). To test whether impaired Notch signaling contributes to vascular abnormalities in EC-iDKO mice, we crossed EC-iDKO with mice carrying a transgene encoding the active form of Notch, Notch intracellular domain (NICD), to create *Epn1$^{fl/fl}$Epn2$^{-/-}$VEcad-ER^{T2} Cre* and NICD transgenic mice (EC-iDKO:NICD) (Supplemental Figure 1G). These mice express the transgene only in ECs when Cre recombinase is activated owing to a floxed stop codon preceding the start codon of NICD (Supplemental Figure 1G). Expression of NICD and deletion of epsin 1 were detected by Western blot analysis of ECs isolated from EC-iDKO:NICD mice after tamoxifen administration, and levels of NICD were similar in EC-iDKO:NICD and WT (Supplemental Figure 1H), suggesting that tamoxifen-induced expression of the NICD transgene rescued the reduction of NICD caused by loss of epsins 1 and 2. However, tumors implanted in EC-iDKO:NICD mice exhibited retarded growth that was similar to that of those in EC-iDKO mice (Figure 4A). Furthermore, augmented Evans blue dye extravasation in response to VEGF caused by loss of endothelial epsins 1 and 2 cannot be rescued by restoring Notch signaling (Figure 4B). These results suggest that the heightened vascular leaking phenotype in EC-iDKO mice caused by increased VEGF signaling is independent of Notch activation. This finding is consistent with VEGF being upstream of Notch signaling (22, 23).

Despite the fact that in vivo rescue of Notch function does not compensate for the increased vascular leak and retarded tumor growth in EC-iDKO mice, we cannot rule out a contribution of loss-of-function of Notch to the marked increase in VEGF signaling in DKO MECs (19, 24, 25). To address this, we expressed NICD in DKO MECs by transfecting a mammalian expression vector containing the NICD-coding region in DKO MECs to rescue defective Notch signaling and examined VEGF-induced signaling. NICD expression restored Notch signaling in DKO MECs, as is evident by the enhanced expression of *Hey2* and *Hes1* (Figure 4C), downstream targets of Notch signaling. However, neither mRNA (Figure 4C) nor protein levels of VEGFR2 (Figure 4D) were affected by NICD expression. Furthermore, NICD expression in DKO MECs did not significantly alter VEGFR2 phosphorylation or total VEGFR2 levels (Figure 4D) compared with DKO MECs. Likewise, exogenous expression of a full-length Notch in DKO MECs in the presence or absence of a γ-secretase inhibitor did not change VEGFR2 phosphorylation (Figure 4E and Supplemental Figure 6A) as compared with DKO MECs alone. Blocking Notch signaling in WT MECs by incubation with a γ-secretase inhibitor also produced no significant change in VEGFR2 phosphorylation or total VEGFR2 levels (Figure 4F). Although no detectable Notch signaling was observed in HUVECs (Supplemental Figure 6B), epsin deficiency still caused aberrant upregulation of VEGF signaling (Figure 3B). Accordingly, regardless of the presence or absence of functional Notch, loss of epsins 1 and 2 caused elevated VEGFR2 signaling. These results support the idea that the observed effect of VEGFR2 is independent of Notch signaling (11).

VEGF induces VEGFR2 ubiquitination, and epsins 1 and 2 interact selectively with ubiquitinated VEGFR2 via UIM. VEGFR2 can be ubiquitinated upon VEGF stimulation (26). The presence of ubiquitin interacting motifs (UIMs) in epsin structure (Figure 5A) raised the possibility that epsin interacts with ubiquitinated VEGFR2 to selectively mediate its internalization. To address this, we first investigated whether epsin interacts with VEGFR2 by coimmunoprecipitation in bovine aorta ECs (BAECs), where epsin 1, epsin 2, and VEGFR2 are endogenously expressed. BAECs were serum starved overnight before being stimulated with 50 ng/ml VEGF for 0, 2, 5, 15, and 30 minutes. Subsequently, cell lysates were immunoprecipitated using anti–epsin 1 antibodies, and the levels of VEGFR2 in the starting lysates and immunoprecipitates were analyzed by Western blotting (Figure 5B). VEGF stimulation, which induced the degradation of VEGFR2, as seen by the decrease in the VEGFR2 signal from 0 to 30 minutes (Figure 5B), also induced the interaction of VEGFR2 with endogenous epsin 1 (Figure 5B) and epsin 2 (Figure 5C). The maximum interaction occurred at 2 minutes after addition of VEGF (Figure 5, B and C). We further tested the interaction in 293T cells where VEGFR2 is not endogenously expressed. FLAG-tagged epsin 1 and VEGFR2-transfected 293T cells were treated with 50 ng/ml VEGF for 5 minutes, and cell lysates were then processed for reciprocal coimmunoprecipitations using either anti-FLAG (Figure 5D) or anti-VEGFR2 (Figure 5E) antibodies. In each case, epsin 1 coprecipitated with VEGFR2. Western blotting analysis of coimmunoprecipitations with an anti–phospho-VEGFR2 antibody further substantiated that epsin 1 binds activated VEGFR2 (Figure 5D).

To test whether epsin interacts with ubiquitinated VEGFR2, BAECs were stimulated with 50 ng/ml VEGF for 0, 5, and 15 minutes and cell lysates were extracted using RIPA buffer immunoprecipitated with anti-VEGFR2 and Western blotted using anti-ubiquitin antibodies. In agreement with previous reports (26, 27), we observed strong, but transient, ubiquitination of VEGFR2 at 5 minutes (Figure 5F). Binding of epsin to ubiquitinated VEGFR2, was assessed by sequential coimmunoprecipitations from VEGF-treated 293T cells coexpressing FLAG-tagged epsin 1 and VEGFR2. First, RIPA lysates were immunoprecipitated using anti-FLAG antibodies. Next, immunoprecipitates were solubilized with SDS, and, after "renaturation" by addition of excess RIPA buffer, processed for a second round of immunoprecipitation using anti-VEGFR2 antibodies. Western blots by anti-ubiquitin antibodies demonstrated that epsin 1 coprecipitated ubiquitinated VEGFR2 (Figure 5G). To determine whether binding of ubiquitinated VEGFR2 to epsins requires the epsin UIM (Figure 5A), we used an epsin 1 mutant lacking the UIM domain (epsin 1 ΔUIM; Figure 5, A and H). 293T cells coexpressing HA-tagged epsin 1 or epsin 1 ΔUIM and VEGFR2 were treated with VEGF for 5 minutes. Coimmunoprecipitation experiments from these cells using anti-HA antibodies demonstrated that deletion of the UIM completely abolished binding of VEGFR2 to epsin 1 (Figure 5H). These results support the hypothesis that the UIM-ubiquitin interaction is critically required for the interaction between epsin and VEGFR2. Since typically the fraction of a given surface protein that is in the ubiquitinated state at any given time is very low, it remains possible that interactions other than the UIM-ubiquitin interaction, but induced by this interaction, may account for the robust coprecipitation observed.

Loss of endothelial epsin 1 and 2 results in impaired VEGF-induced VEGFR2 internalization and degradation. The role of epsin in the endocytosis of VEGFR2 was assessed by monitoring endocytic trafficking of VEGFR2 in MECs in response to VEGF stimulation using confocal microscopy. WT or DKO MECs were serum starved overnight before being stimulated with VEGF for 0 to 20 minutes. Total and/or internalized VEGFR2 was then visualized after fixation and permeabilization by direct imaging of VEGFR2-bound biotinylated VEGF/streptavidin–Alexa Fluor 488 to detect cell surface and internalized VEGFR2 (Figure 6A). Samples were

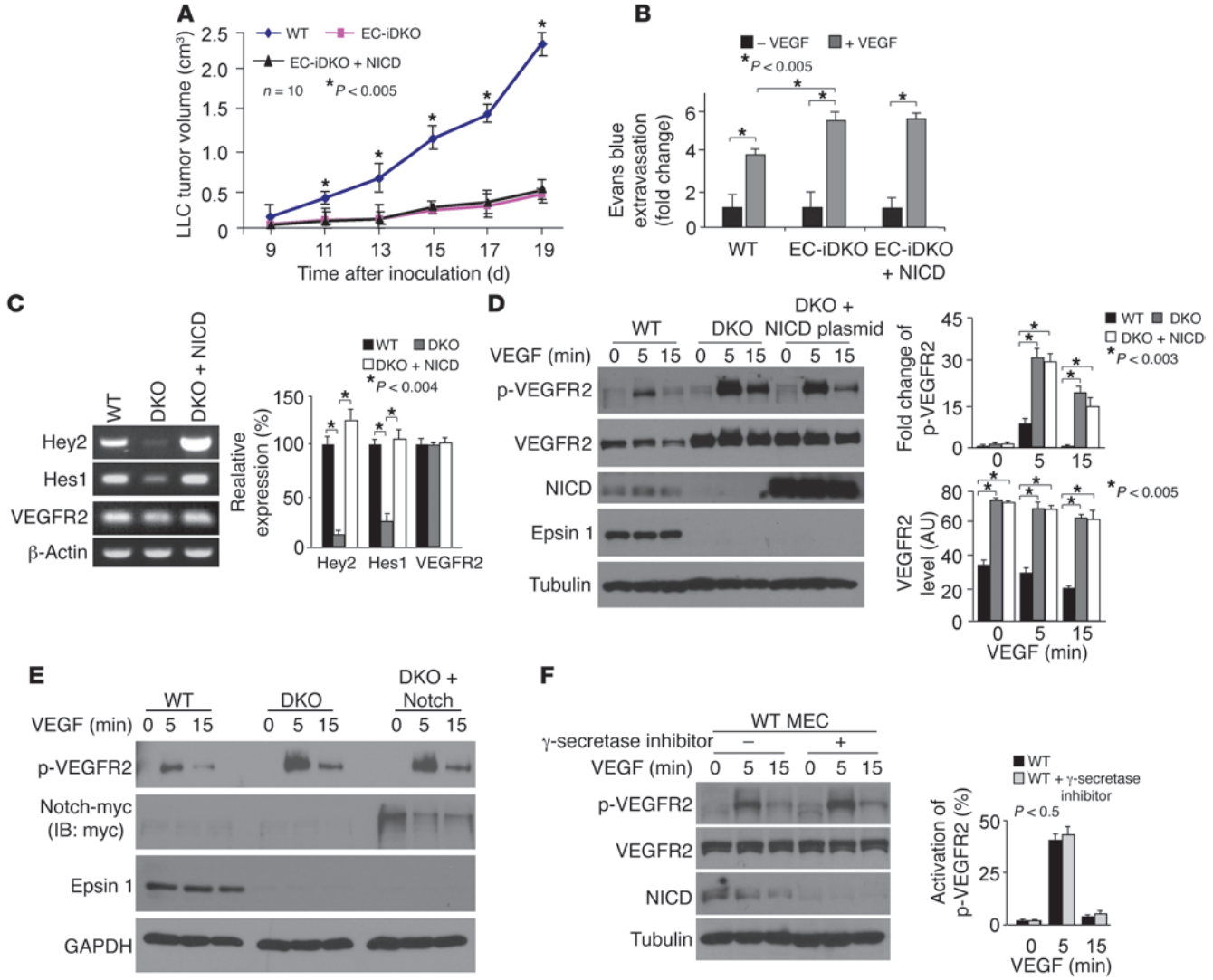

Figure 4

Restoring Notch function does not rescue retarded tumor growth, augmented vascular leak, and elevated VEGFR2 signaling due to loss of endothelial epsins 1 and 2. (**A**) LLC tumor growth in EC-iDKO, EC-iDKO+NICD, or WT mice from day 9 through 19 after inoculation of LLC cells. (**B**) VEGF-induced augmented ear vessel permeability in WT, EC-iDKO, or EC-iDKO+NICD mice revealed by Evans blue dye extravasation. (**C**) RT-PCR showing the mRNA expression of *Hey2*, *Hes1*, and *VEGFR2* in WT, or DKO MECs transfected with an empty vector or a mammalian expression vector containing NICD coding region for 24 hours. Quantification of relative expression normalized according to β-*actin* is on right. (**D**) WT or DKO MECs transfected as in **C** were starved and stimulated with VEGF-A (50 ng/ml) and analyzed by Western blotting. Quantification of total or phosphorylated VEGFR2 is shown on right. (**E**) WT or DKO MECs transfected with an empty vector or a full-length Notch-myc plasmid for 24 hours were starved and stimulated with VEGF-A (50 ng/ml) and analyzed by Western blotting. (**F**) WT MECs were treated with or without γ-secretase inhibitor (10 μM) for 24 hours followed by stimulation with VEGF-A (50 ng/ml) and analyzed by Western blotting. Quantification of phosphorylated VEGFR2 is on right. $n > 5$ per group in all panels.

costained by immunofluorescence for various endocytic markers including clathrin, epsin 1, EEA1, and LAMP1 (Figure 6, A and B, and Supplemental Figure 7A). Strong colocalization of VEGFR2 with clathrin (Supplemental Figure 7A) and epsin 1 (Figure 6A) was observed at early stages of VEGFR2 endocytosis after addition of VEGF (see the 2 minute time point). At 10 minutes, internalized VEGFR2 colocalized primarily with the endosomal marker EEA1 (Figure 6A) and at 20 minutes with the lysosomal marker LAMP1 (Figure 6A). This data supports VEGF-dependent internalization of VEGFR2 by clathrin- and epsin-dependent endocytosis with subsequent targeting to lysosomes for degradation as previously reported (26, 27). However, these colocalizations and corresponding endocytic trafficking of VEGFR2 were not observed in DKO MECs (Figure 6A), indicating that loss of epsins 1 and 2 in ECs results in impaired VEGFR2 internalization.

We further confirmed the defective endocytosis of VEGFR2 in DKO MECs biochemically. WT or DKO MECs were surface labeled with cleavable biotin at 4°C to tag surface-exposed VEGFR2. Cells were then shifted to 37°C and exposed to 50 ng/ml VEGF for 5 or 20 minutes. This was followed by cleavage of biotin moieties remaining at the cell surface, so that only the protected internalized proteins retained biotin. Lysates from these cells were

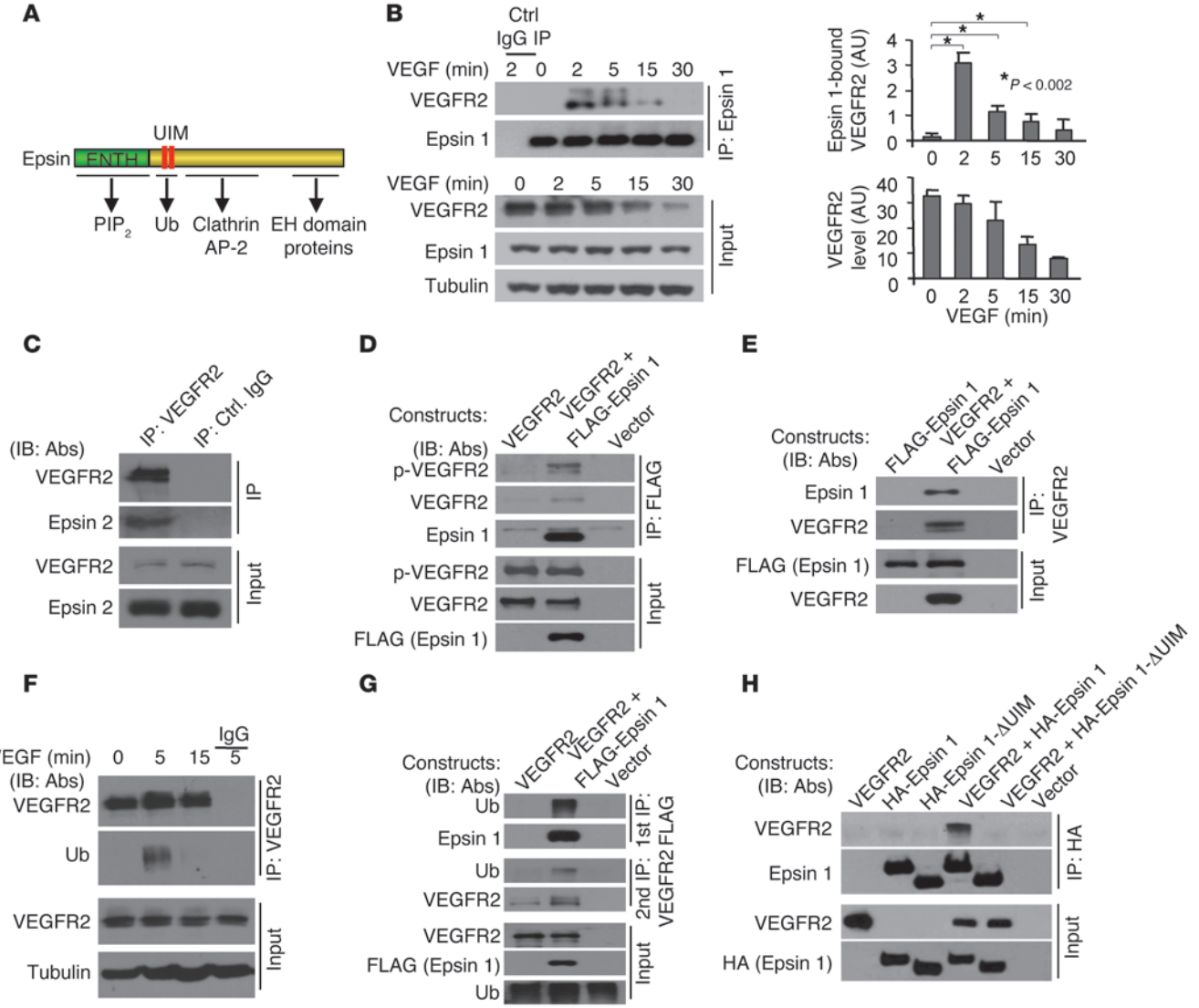

Figure 5

VEGF induces VEGFR2 ubiquitination and binding to epsins 1 and 2, and interaction of epsin and VEGFR2 requires epsin UIM. (**A**) Schematic drawing of epsin depicts interactions between ENTH domain and PI(4,5)P2, UIM, and ubiquitin, COOH-terminal domain and clathrin, AP-2, and EH domain-containing proteins. (**B**) Lysates from BAECs stimulated with VEGF-A were immunoprecipitated with anti–epsin 1 or control IgG and Western blotted with anti-VEGFR2. Quantifications showing epsin 1 bound to VEGFR2 and total VEGFR2 are on right. (**C**) Lysates from BAECs stimulated with VEGF-A for 2 minutes were immunoprecipitated with anti-VEGFR2 or control IgG and Western blotted with anti–epsin 2. (**D**) Lysates from HEK 293T cells expressing indicated plasmids stimulated with VEGF-A for 2 minutes were immunoprecipitated with anti-FLAG and Western blotted with indicated antibodies. (**E**) Lysates from HEK 293T cells expressing indicated plasmids stimulated with VEGF-A for 2 minutes were immunoprecipitated with anti-VEGFR2 and Western blotted with indicated antibodies. (**F**) Lysates from BAECs stimulated with VEGF-A were immunoprecipitated with anti-VEGFR2 or control IgG and Western blotted with the indicated antibodies. (**G**) Lysates from HEK 293T cells expressing indicated plasmids stimulated with VEGF-A for 5 minutes were first immunoprecipitated with anti-FLAG and Western blotted with indicated antibodies. Immunoprecipitates were eluted and subjected to a second immunoprecipitation with anti-VEGFR2 and Western blotted with indicated antibodies. (**H**) Lysates from HEK 293T cells expressing indicated plasmids were stimulated with VEGF-A for 5 minutes and were immunoprecipitated with anti-HA and Western blotted with antibodies indicated. 50 ng/ml VEGF-A was used in **B**–**H**.

incubated with streptavidin beads, and the bound, internalized VEGFR2 fraction was measured by Western blotting with antibodies directed to VEGFR2 (Figure 6B). A prominent portion of internalized VEGFR2 was detected in WT MECs at 5 minutes. At 20 minutes, this intracellular pool of VEGFR2 was reduced, presumably due to lysosomal degradation (Figure 6B). In contrast, virtually no internalized VEGFR2 was detected either at 5 or 20 minutes in DKO MECs (Figure 6B), suggesting that loss of epsin 1 and epsin 2 abolishes the endocytosis and degradation of VEGFR2 induced by VEGF stimulation.

Importantly, incubation of serum starved WT or DKO MECs with biotinylated VEGF-A/streptavidin–Alexa Fluor 488 in the additional presence of transferrin labeled with Alexa Fluor 594 for 0 and 10 minutes at 37°C revealed an absence of VEGF internal-

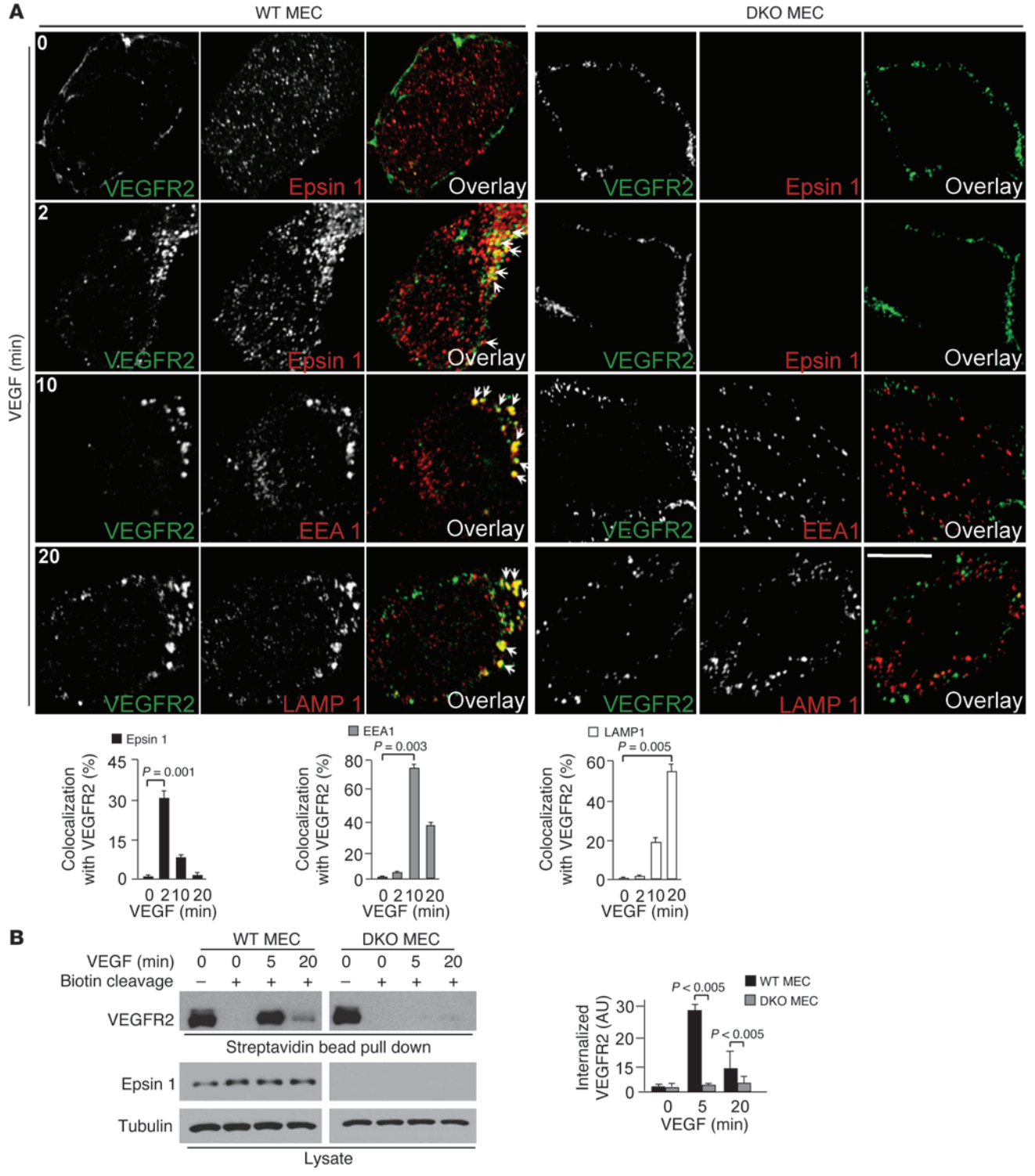

Figure 6

Lack of endothelial epsins 1 and 2 impairs VEGF-induced VEGFR2 endocytosis (**A**) WT or DKO MECs were incubated with biotinylated VEGF-A/streptavidin–Alexa Fluor 488 at 4°C for 30 minutes, shifted to 37°C for 0 to 20 minutes, and processed for immunofluorescence. Colocalization of biotinylated VEGF-A/streptavidin–Alexa Fluor 488–labeled VEGFR2 with Alexa Fluor 594–labeled epsin 1 at 2 minutes, EEA1 at 10 minutes, and LAMP1 at 20 minutes seen by confocal microscopy. Arrows indicate colocalization of the 2 proteins. Quantification of colocalized proteins is on right. (**B**) Cell surface of WT or DKO MECs was labeled with cleavable biotin at 4°C for 30 minutes, incubated with VEGF-A (50 ng/ml) at 37°C for the time points as indicated, followed by cleavage of surface biotin; internalized biotinylated VEGFR2 was determined by streptavidin bead pull-down and Western blotted with anti-VEGFR2. Quantification of internalized VEGFR2 is on right. $n > 5$ per group in all panels. Scale bar: 10 μm (**A**).

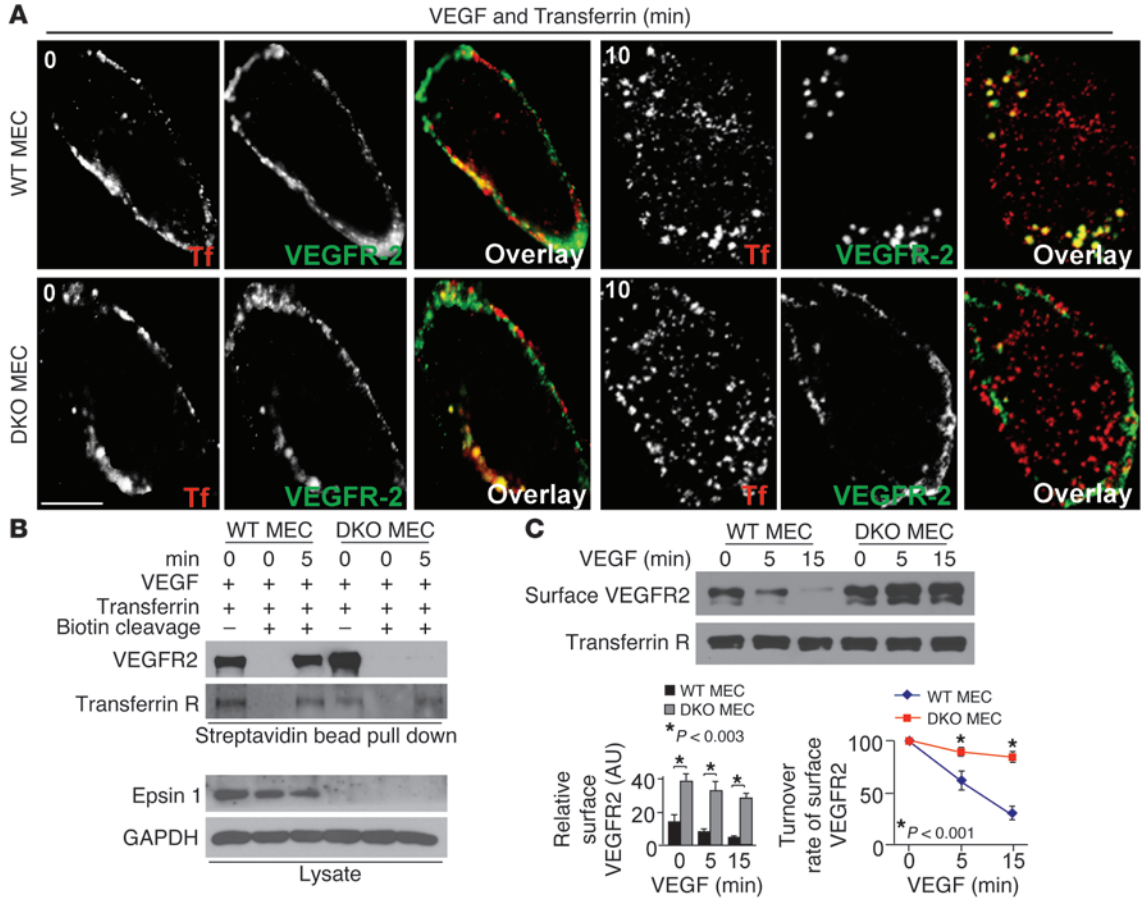

Figure 7

Loss of endothelial epsins 1 and 2 inhibits endocytosis of VEGFR2 but not transferrin receptor, leading to surface accumulation of VEGFR2. (**A**) WT or DKO MECs were incubated with 100 ng/ml of biotinylated VEGF-A/streptavidin–Alexa Fluor 488 and 10 μg/ml transferrin Alexa Fluor 594 conjugate at 4°C for 30 minutes, shifted to 37°C for 0 to 10 minutes, and processed for immunofluorescence. (**B**) Cell surface of WT or DKO MECs was labeled with cleavable biotin at 4°C for 30 minutes, incubated with VEGF (50 ng/ml) and holo-transferrin (10 μg/ml) for 0 to 5 minutes, followed by cleavage of surface biotin, and internalized biotinylated VEGFR2 and transferrin receptor were determined by streptavidin bead pull-down and Western blotting with the indicated antibodies. (**C**) WT or DKO MECs were incubated with VEGF-A (50 ng/ml) for the times indicated, and cell-surface VEGFR2 was labeled by cell-surface biotinylation, and analyzed by streptavidin bead pull-down followed by Western blotting with antibodies indicated. Turnover rate of cell-surface VEGFR2 was plotted based on the expression of cell-surface VEGFR2 after VEGF-A treatment normalized against nontreated samples. $n > 5$ per group in all panels. Scale bar: 10 μm (**A**).

ization but normal transferrin internalization in DKO MECs (Figure 7A), arguing against a global block of endocytosis and thus in agreement with previous analysis of epsin 1 and epsin 2 DKO or double-knockdown cells (9, 28). These results were confirmed biochemically. WT or DKO MECs were surface labeled with cleavable biotin at 4°C to tag both surface-exposed VEGFR2 and transferrin receptor. Cells were then shifted to 37°C, exposed to 50 ng/ml of VEGF or 10 μg/ml transferrin for 5 minutes, and treated as described above to retain biotin only in the internalized proteins. After incubation of cell lysates with streptavidin beads, the bound, internalized VEGFR2 and transferrin receptors were measured by Western blotting with specific antibodies to VEGFR2 and transferrin receptor, respectively. This analysis showed normal internalization of transferrin receptor but defective endocytosis of VEGFR2 in DKO MECs (Figure 7B).

Defective internalization of VEGFR2 in DKO cells predicts an accumulation of VEGFR2 on the cell surface. To test this, cell-surface levels of VEGFR2 before and after VEGF stimulation in WT and DKO cells were assessed. MECs were starved overnight and then treated with 50 ng/ml of VEGF for 0, 5, and 15 minutes at 37°C to allow internalization of cell-surface VEGFR2. Subsequently, cells were incubated with noncleavable biotin to label remaining cell surface VEGFR2, cell lysates were affinity purified on streptavidin beads, and bound material was analyzed by Western blotting using anti-VEGFR2 antibodies to visualize cell-surface VEGFR2 (Figure 7C). Lack of epsin 1 and epsin 2 produced a 2-fold increase in cell-surface VEGFR2 even in the absence of VEGF stimulation (Figure 7C). This elevated VEGFR2 level was not due to increased transcription of VEGFR2, as a similar VEGFR2 mRNA levels were detected in WT or DKO MECs by RT-PCR (Figure 3D). In agreement with this result, VEGF treatment resulted in a reduction of surface VEGFR2 at 5 and 15 minutes in WT but not in DKO MECs (Figure 7C).

Next, we investigated the role of epsin 1 and epsin 2 in the endocytosis and degradation of VEGFR2 using a knockdown approach. This approach produces an acute downregulation of epsins 1 and

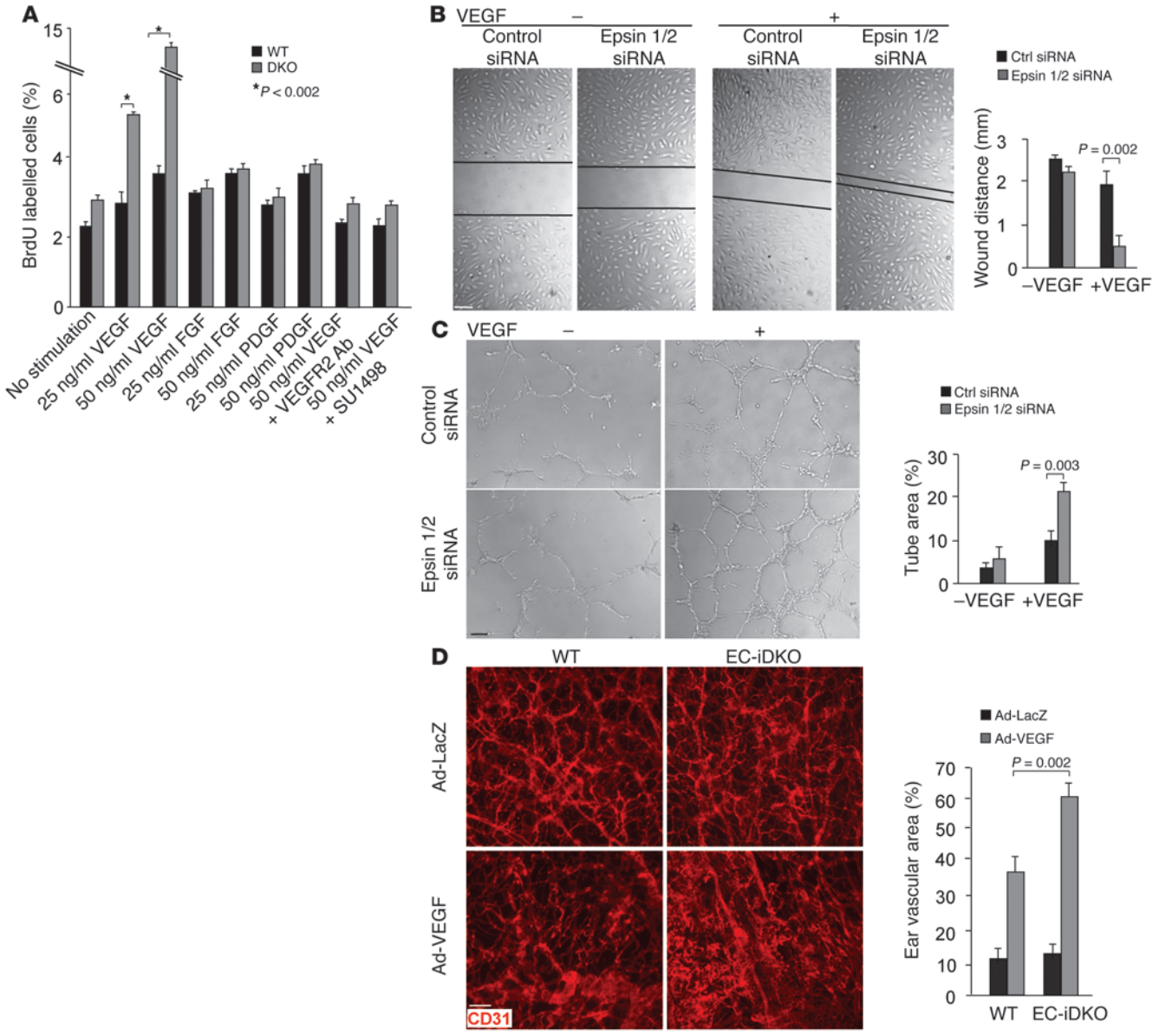

Figure 8

Loss of endothelial epsins 1 and 2 augments EC proliferation and migration and increases VEGF-induced ear neovascularization in mice. (**A**) VEGF but not FGF or PDGF increased proliferation of DKO MECs relative to WT MECs measured by BrdU labeling. The increase is abrogated by inhibitors of VEGFR2. (**B**) HUVECs transfected with control or epsin 1 and 2 siRNAs were subjected to a monolayer "wound injury" assay in the absence or presence of VEGF-A (50 ng/ml) for 12 hours. (**C**) HUVECs transfected with control or epsin 1 and 2 siRNAs were cultured on Matrigel for 16 hours in the absence of presence of VEGF-A (50 ng/ml). (**D**) Adenovirus encoding $VEGF_{164}$ (Ad-VEGF) or β-galactosidase (Ad-LacZ) (1×10^9 PFU) was intradermally injected into the mouse ears. Ear vasculature was visualized by whole-mount staining with PE-conjugated anti-CD31. Quantification of vessel density is on right. $n > 5$ per group in all panels. Scale bars: 50 μm (**B**–**D**).

2 to rule out a possible effect of compensation in the tumor endothelium of EC-iDKO due to chronic deletion of epsins 1 and 2. HUVECs were transfected with either control or epsin 1 and epsin 2 siRNAs (Supplemental Figure 7B), stimulated with 50 ng/ml VEGF for 0, 5, 15 minutes, and incubated with anti-VEGFR2 antibodies at 4°C for 30 minutes followed by incubation with secondary antibodies conjugated to Alexa Fluor 488 at 4°C for 30 minutes. Bound antibodies were then quantified by FACS analysis. Increased surface accumulation of VEGFR2 was observed in epsin-deficient HUVECs when compared with control HUVECs (Supplemental Figure 7, C–E). VEGF stimulation resulted in a prominent decrease in the cell-surface pool of VEGFR2 in control HUVECs at 5 and 15 minutes (Supplemental Figure 7, C–E). In contrast, very little change in the cell-surface pool of VEGFR2 was detected in epsin-deficient HUVECs upon VEGF stimulation (Supplemental Figure 7, C–E), supporting that epsin 1 and epsin 2 play a key role in the endocytosis and thus degradation of VEGFR2.

Interestingly, VEGF did not promote the endocytosis of VEGFR1, another VEGFR family member, which has high affinity for VEGF but weak tyrosine kinase activity and is thought to work

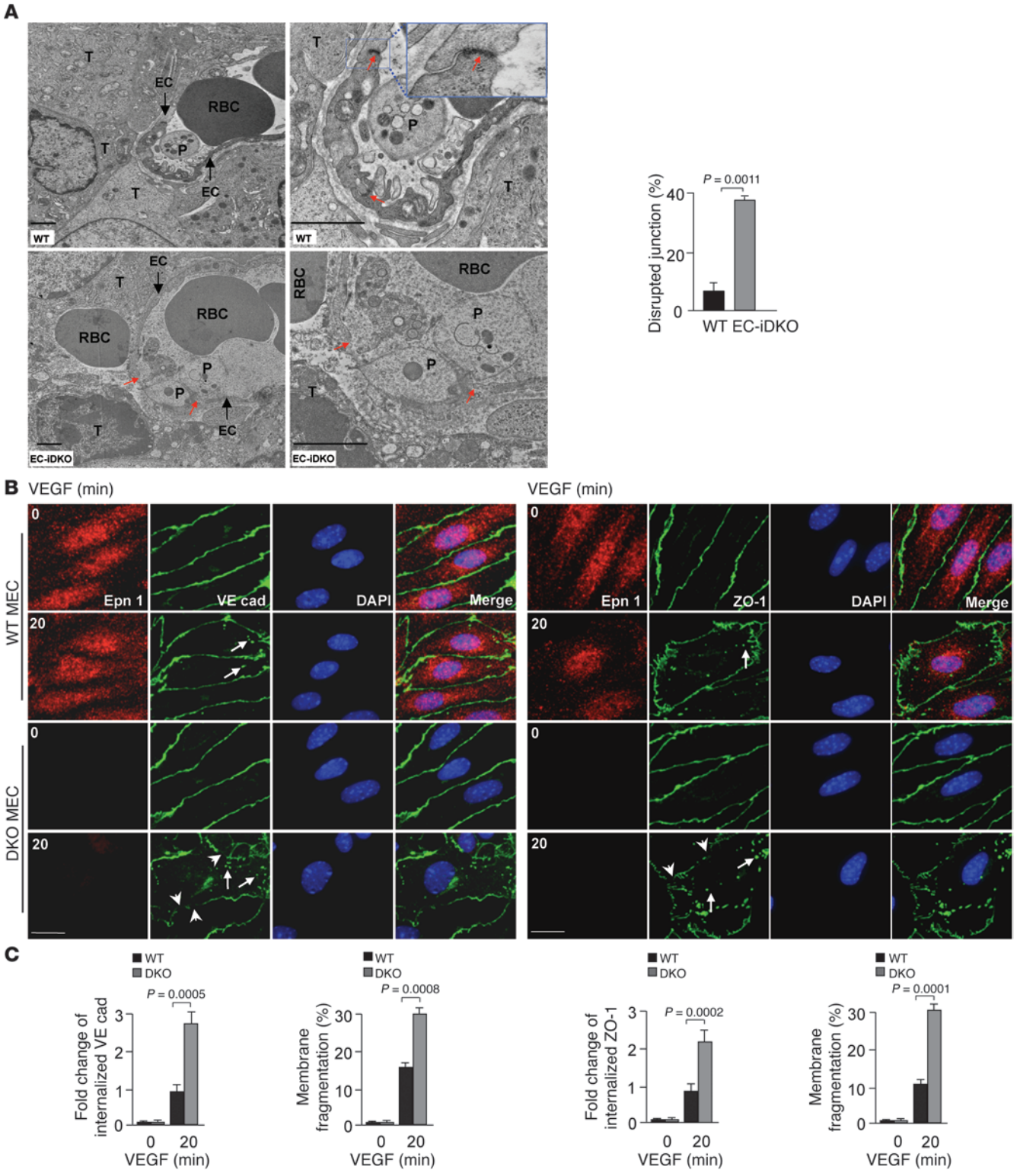

Figure 9

Disrupted endothelial junctions in tumor vessels and mouse primary ECs lacking endothelial epsins 1 and 2. (**A**) Transmission electron micrographs show large open intercellular junctions in EC-iDKO tumor vessels compared with WT tumor vessels. T, tumor cell; P, platelet. Red arrows indicate open EC junctions. Percentages of disrupted junctions in WT and EC-iDKO tumor vessels are on right. (**B** and **C**) Confocal images of WT or DKO MECs stimulated with 50 ng/ml VEGF-A followed by immunostaining for VE-cadherin (**B**) or ZO-1 (**C**) revealed VEGF-induced augmented internalization of VE-cadherin or ZO-1 (arrows) and highly disrupted intercellular junctions (arrowheads) in DKO MECs. Quantifications of internalized VE-cadherin or ZO-1, and membrane fragmentation are on right. n = 12 (**A**); 15 (**B** and **C**). Scale bars: 1.5 μm (**A**); 10 μm (**B** and **C**).

as a sink for VEGF either as a membrane-bound or cleaved form, regardless of the presence or absence of epsin 1 and epsin 2 (Supplemental Figure 8, A and B). VEGFR3, which is highly expressed in lymphatic ECs, is only weakly expressed in HUVECs or MECs (Supplemental Figure 8C and ref. 29).

Loss of endothelial epsins 1 and 2 augments EC proliferation and migration and produces abnormal angiogenesis in response to VEGF. Recent evidence demonstrates a close link between VEGFR2 internalization and signaling (30), raising the possibility that epsin deficiency results in abnormal VEGFR2 signaling and endothelial cellular responses required for angiogenesis. We hypothesized that angiogenic cellular responses to VEGF should be enhanced by epsin deficiency. We examined endothelial cellular responses including cell proliferation and migration in epsin-deficient ECs in response to VEGF by BrdU labeling, wound closure, and tube formation assays. We observed that VEGF, but not FGF or PDGF, greatly enhanced the proliferation of DKO MECs relative to WT MECs, as measured by BrdU labeling (Figure 8A). This stimulation was abrogated by inhibiting VEGFR2 using anti-VEGFR2 antibodies or the VEGFR2 inhibitor SU1498 (Figure 8A). Similarly, VEGF markedly increased proliferation and migration of HUVECs lacking epsins 1 and 2, as measured by the wound closure assay in cell monolayers (Figure 8B) and the network formation in Matrigel-based tube formation assay (Figure 8C). Enhanced in vitro angiogenesis from loss of epsins 1 and 2 is consistent with the elevated VEGF signaling and may contribute to abnormal tumor angiogenesis, including enlarged vessels observed in EC-iDKO tumors. We also performed VEGF-induced ear angiogenesis in EC-iDKO mice to determine the role of epsins 1 and 2 in regulating VEGF/VEGFR2–dependent angiogenesis in vivo (16). Adenovirus encoding $VEGF_{164}$ or β-galactosidase was injected intradermally into the ears. VEGF-induced angiogenesis was accessed by whole-mount staining with anti-CD31 (Figure 8D). We observed that VEGF-induced in vivo angiogenesis was dramatically augmented in EC-iDKO compared with WT mice, consistent with our in vitro angiogenesis results.

Lack of endothelial epsins 1 and 2 results in disrupted endothelial junctions. VEGF was first discovered as a potent vascular permeability factor (VPF) (31, 32). We hypothesize that heightened VEGF signaling in tumor ECs produces prominent hyper-permeable tumor vessels phenotype in EC-iDKO mice. To test this, we performed transmission electron microscopy (TEM). TEM micrographs showed that 2- to 4-μm–wide open intercellular junctions were frequently present in EC-iDKO tumor vessels (Figure 9A). This was accompanied by marked leaking of blood cells (Figure 9A). In contrast, the less leaky WT tumor vessels showed numerous intact intercellular junctions (Figure 9A). EC-iDKO tumor endothelium also exhibited increased fenestration and enlarged vesiculo-vacuolar organelles (Supplemental Figure 9A and refs. 31, 32). Semi-thin sections of EC-iDKO tumor vessels revealed prominent leakage of blood cells, with massive necrotic regions in the surrounding tumor (Supplemental Figure 9B).

VE-cadherin is critical for maintaining adherens junctions between ECs (33). One characteristic of VEGF-induced vascular permeability is the phosphorylation of VE-cadherin on tyrosines or serine, which leads to the internalization of VE-cadherin and the destabilization of adherens junctions (33, 34). As shown in Figure 9B, after treatment with VEGF, adherens junctions in DKO MECs were more jagged in appearance compared with WT, indicating disruption of the junctions. Internalized VE-cadherin puncta were visible in both groups of cells, but DKO MECs displayed more puncta correlating with larger membrane gaps and fragmentations (Figure 9B). The tight-junction marker ZO-1 also revealed augmented tight-junction disruption in DKO MECs upon VEGF treatment (Figure 9C), suggesting that enhanced VEGF signaling in DKO MECs induces elevated endocytosis of the tight junction proteins, including ZO-1 and Occludin, and thus increases vascular permeability (35). These results indicate an underlying mechanism for increased permeability that is dependent on the loss of endothelial epsins 1 and 2.

Discussion

Our results demonstrate that genetic ablation of endothelial epsins 1 and 2 resulted in excessive and prolonged VEGFR2 signaling in tumor vasculature. These effects result in leaky vessels with enlarged diameters and highly chaotic morphology. These vascular changes correlate with, and thus may be responsible for, retarded tumor growth. Furthermore, we demonstrate that epsins 1 and 2 interact with ubiquitinated VEGFR2 upon VEGF stimulation to selectively mediate the endocytosis and degradation of VEGFR2. Such interaction requires the ubiquitination of the receptor and the UIM motifs of epsins 1 and 2. We conclude that endothelial epsins 1 and 2 are required for functional tumor angiogenesis and tumor growth by restricting excessive VEGF signaling.

Angiogenesis is essential for tumor growth and metastasis. VEGF is one of the most potent promoters of angiogenesis. The need for oxygen and nutrients triggers tumor cells to release VEGF, which leads to robust tumor angiogenesis. Tumor vasculature is known to be leaky and tortuous. However, these newly formed vessels are sufficient to provide the tumor with oxygen and nutrients, especially in the early phase of tumor growth. In addition, these new vessels may facilitate tumor cells spreading through blood circulation to other parts of the body. Sustained angiogenesis is a hallmark of most, if not all, cancers. Accordingly, antiangiogenic therapy has been widely used to treat a broad spectrum of cancers (13). Our data show that even enhanced VEGF signaling, as produced by epsin 1 and 2 deficiency, results in a decreased tumor growth due to impaired tumor angiogenesis, contributing to tumor-resistant phenotype. The retarded tumor growth by loss of endothelial epsins 1 and 2 is consistently observed in several types of tumor models, most of them known to have robust tumor angiogenesis. These results suggest novel strategies in the development of antiangiogenic therapies.

Most of current anti-VEGF drugs have various extents of side complications, such as bleeding or organ failure, because some organ vessels, such as glomerular microvessels, are dependent on basal VEGF levels for their physiological function (36, 37). Our epsin EC-iDKO or EC-DKO mouse models of epsin deficiency are indistinguishable from those of WT mice, exhibiting no gross abnormalities. Similarly, we fail to observe any significant structural and functional changes in organ vessels, including glomerulus microvessels, as demonstrated by FITC-dextran vascular perfusion assays under normal conditions (Supplemental Figure 10), indicating that lack of endothelial epsins 1 and 2 after the vasculature has developed has minimal impact on quiescent vessels and vessels undergoing remodeling in normal tissues. Although EC-iDKO mice appear normal under physiological conditions, these mice have lost epsins 1 and 2 selectively in their endothelium. Thus, future studies addressing the effect of inhibiting epsin function in non-ECs in adult animals are warranted. Furthermore,

it would be useful to determine whether physiological angiogenesis, such as wound healing, might also be affected by endothelial deficiency of epsins 1 and 2.

Our in vitro assays indicate that loss of epsins 1 and 2 selectively affects clearance of activated VEGFR2 through a specific ubiquitination-UIM–dependent mechanism, but not other angiogenic factor pathways in ECs. Moreover, loss of epsins 1 and 2 has no impact on housekeeping transferrin uptake, suggesting that epsins 1 and 2 are only important for internalization of a unique set of activated receptors. It has been shown that diminished internalization and degradation of some receptor tyrosine kinases results in heightened signaling and enhanced tumor growth. Most notably, upregulation of EGFR signaling promotes development of several types of cancer. Although loss of epsins 1 and 2 does not affect EGFR internalization (9) and downstream signaling in our cellular system (Figure 3G), future studies should shed light on whether epsins 1 and 2 might be important for internalization and downregulation of other receptors crucial for tumor growth.

Collectively, our findings demonstrate that prolonged VEGF signaling in the absence of endothelial epsins 1 and 2 produces leaky, defective tumor angiogenesis, contributing to tumor growth retardation. This result suggests that tumor vasculature also requires stringently balanced VEGF signaling to provide sufficient productive angiogenesis for tumor development. In addition, our work shows that endothelial epsins 1 and 2 may play a key role in negatively regulating VEGF signaling by promoting VEGFR2 internalization and degradation. Therefore, our data suggest a potential antiangiogenic strategy, which is to promote local excessive VEGF signaling by loss of endothelial epsins 1 and 2. This new pro-VEGF signaling approach might be beneficial for patients with tumors that are resistant to anti-VEGF therapies.

Methods

Generation of conditional Epn1$^{fl/fl}$ and EC-specific DKO mice. We reported a strategy for the generation of mice globally deficient in epsins 1 and 2 (9). We used a similar strategy with modifications to create a conditional KO of epsin 1 mice (*Epn1$^{fl/fl}$*). *Epn1$^{fl/fl}$* were mated with *Epn2$^{-/-}$* to generate *Epn1$^{fl/fl}$Epn2$^{-/-}$* mice, which are on a C57BL/6J congenic background. Tamoxifen-inducible EC-specific DKO mice (EC-iDKO) were obtained by crossing *Epn1$^{fl/fl}$Epn2$^{-/-}$* mice with *VEcad-ER^{T2} Cre* mice on a C57BL/6J background, which inactivates the epsin 1 gene specifically in ECs upon tamoxifen administration. To induce postnatal deletion of endothelial epsin 1, we administered 4-hydroxytamoxifen (150 μg/30 g of body weight) by i.p. injection into 10-week-old WT or *Epn1$^{fl/fl}$Epn2$^{-/-}$VEcad-ER^{T2} Cre* mice with or without the NICD transgene. Injections were performed once per day for 5 to 7 consecutive days, followed by a 5- to 7-day resting period to obtain WT, EC-iDKO or EC-iDKO:NICD mice. EC-DKO were generated by crossing *Epn1$^{fl/fl}$Epn2$^{-/-}$* mice with *VEcad-Cre* mice on a C57BL/6J background. C57BL/6J WT mice bred with Cre-transgenic mice or other transgenic mice were used as WT controls throughout in the study.

Statistical analysis. Data were shown as mean ± SEM. Data were analyzed by the 2-tailed Student's *t* test or ANOVA, where appropriate. The Wilcoxon signed-rank test was used to compare data that did not satisfy the Student's *t* test or ANOVA. $P \leq 0.05$ was considered significant.

Study approval. All animal studies were performed in compliance with institutional guidelines and were approved by Institutional Animal Care and Use Committee (IACUC), Oklahoma Medical Research Foundation.

Additional methods are provided in Supplemental Methods.

Acknowledgments

We thank Rodger McEver and Holger Gerhardt (LRC-Cancer Research, United Kingdom) for insightful comments, and Shawn Ferguson for helpful discussions. We thank Hendra Setiadi and Cindy Carter for providing HUVECs. We thank LiJuan Li for technical assistance and Tim Nottoli (Yale Cancer Center Animal Genomics Shared Resource) for help with gene targeting. We thank the Oklahoma Medical Research Foundation imaging core for help with the presentation of figures. This work was supported in part by NIH grants R01HL-093242 and P20 RR018758; a grant from the Oklahoma Center for Advanced Science and Technology (OCAST); and a National Scientific Development Grant from the American Heart Association (0835544N to H. Chen); grants from the NIH (NS36251 and DK45735 to P. De Camilli; P01HL085607 to L. Xia; R01 HL085789 and R01 HL109420 to W. Min), and grants from the Associazione Italiana per la Ricerca sul Cancro (AIRC), Association for International Cancer Research – UK (AICR-UK), Telethon, CARIPLO, Interlink, and COFIN/PRIN (to O. Cremona).

Received for publication July 5, 2012, and accepted in revised form September 20, 2012.

Address correspondence to: Hong Chen, Oklahoma Medical Research Foundation, Room 6406, 825 NE 13th Street, Oklahoma City, Oklahoma 73104, USA. Phone: 405.271.2750; Fax: 405.271.3137; E-mail: hong-chen@omrf.org. Or to: Wang Min, Yale University School of Medicine, 10 Amistad Street, Room 401B, New Haven, Connecticut 06520, USA. Phone: 203.785.6047; Fax: 203.787.2293; E-mail: wang.min@yale.edu.

1. Carmeliet P, Jain RK. Molecular mechanisms and clinical applications of angiogenesis. *Nature*. 2011;473(7347):298–307.
2. Olsson AK, Dimberg A, Kreuger J, Claesson-Welsh L. VEGF receptor signalling - in control of vascular function. *Nat Rev Mol Cell Biol*. 2006;7(5):359–371.
3. Rosenthal JA, et al. The epsins define a family of proteins that interact with components of the clathrin coat and contain a new protein module. *J Biol Chem*. 1999;274(48):33959–33965.
4. Chen H, et al. Epsin is an EH-domain-binding protein implicated in clathrin-mediated endocytosis. *Nature*. 1998;394(6695):793–797.
5. Wendland B. Epsins: adaptors in endocytosis? *Nat Rev Mol Cell Biol.* 2002;3(12):971–977.
6. Shih SC, Katzmann DJ, Schnell JD, Sutanto M, Emr SD, Hicke L. Epsins and Vps27p/Hrs contain ubiquitin-binding domains that function in receptor endocytosis. *Nat Cell Biol*. 2002;4(5):389–393.
7. Chen H, De Camilli P. The association of epsin with ubiquitinated cargo along the endocytic pathway is negatively regulated by its interaction with clathrin. *Proc Natl Acad Sci U S A*. 2005;102(8):2766–2771.
8. Ko G, et al. Selective high-level expression of epsin 3 in gastric parietal cells, where it is localized at endocytic sites of apical canaliculi. *Proc Natl Acad Sci U S A*. 2010;107(50):21511–21516.
9. Chen H, et al. Embryonic arrest at midgestation and disruption of Notch signaling produced by the absence of both epsin 1 and epsin 2 in mice. *Proc Natl Acad Sci U S A*. 2009;106(33):13838–13843.
10. Monvoisin A, Alva JA, Hofmann JJ, Zovein AC, Lane TF, Iruela-Arispe ML. VE-cadherin-CreERT2 transgenic mouse: a model for inducible recombination in the endothelium. *Dev Dyn*. 2006;235(12):3413–3422.
11. Benedito R, et al. Notch-dependent VEGFR3 upregulation allows angiogenesis without VEGF-VEGFR2 signalling. *Nature*. 2012;484(7392):110–114.
12. Alva JA, et al. VE-Cadherin-Cre-recombinase transgenic mouse: a tool for lineage analysis and gene deletion in endothelial cells. *Dev Dyn*. 2006; 235(3):759–767.
13. Kerbel RS. Tumor angiogenesis. *N Engl J Med*. 2008; 358(19):2039–2049.
14. Zagzag D, et al. Molecular events implicated in brain tumor angiogenesis and invasion. *Pediatr Neurosurg*. 2000;33(1):49–55.
15. Carmeliet P. Angiogenesis in health and disease. *Nat Med*. 2003;9(6):653–660.
16. Zhang H, et al. AIP1 functions as an endogenous inhibitor of VEGFR2-mediated signaling and inflammatory angiogenesis in mice. *J Clin Invest*. 2008;118(12):3904–3916.
17. Weinstein BM, Lawson ND. Arteries, veins, Notch, and VEGF. *Cold Spring Harb Symp Quant Biol*. 2002; 67:155–162.
18. Phng LK, Gerhardt H. Angiogenesis: a team effort coordinated by notch. *Dev Cell*. 2009;16(2):196–208.
19. Suchting S, et al. The Notch ligand Delta-like 4 negatively regulates endothelial tip cell forma-

tion and vessel branching. *Proc Natl Acad Sci U S A*. 2007;104(9):3225–3230.
20. Overstreet E, Fitch E, Fischer JA. Fat facets and Liquid facets promote Delta endocytosis and Delta signaling in the signaling cells. *Development*. 2004; 131(21):5355–5366.
21. Wang W, Struhl G. Drosophila Epsin mediates a select endocytic pathway that DSL ligands must enter to activate Notch. *Development*. 2004; 131(21):5367–5380.
22. Liu ZJ, et al. Regulation of Notch1 and Dll4 by vascular endothelial growth factor in arterial endothelial cells: implications for modulating arteriogenesis and angiogenesis. *Mol Cell Biol*. 2003;23(1):14–25.
23. Lobov IB, et al. Delta-like ligand 4 (Dll4) is induced by VEGF as a negative regulator of angiogenic sprouting. *Proc Natl Acad Sci U S A*. 2007; 104(9):3219–3224.
24. Ridgway J, et al. Inhibition of Dll4 signalling inhibits tumour growth by deregulating angiogenesis. *Nature*. 2006;444(7122):1083–1087.
25. Noguera-Troise I, Daly C, et al. Blockade of Dll4 inhibits tumour growth by promoting non-productive angiogenesis. *Nature*. 2006;444(7122):1032–1037.
26. Ewan LC, et al. Intrinsic tyrosine kinase activity is required for vascular endothelial growth factor receptor 2 ubiquitination, sorting and degradation in endothelial cells. *Traffic*. 2006;7(9):1270–1282.
27. Duval M, Bedard-Goulet S, Delisle C, Gratton JP. Vascular endothelial growth factor-dependent down-regulation of Flk-1/KDR involves Cbl-mediated ubiquitination. Consequences on nitric oxide production from endothelial cells. *J Biol Chem*. 2003; 278(22):20091–20097.
28. Boucrot E, et al. Membrane fission is promoted by insertion of amphipathic helices and is restricted by crescent BAR domains. *Cell*. 2012;149(1):124–136.
29. Jones D, et al. Functional analyses of the bone marrow kinase in the X chromosome in vascular endothelial growth factor-induced lymphangiogenesis. *Arterioscler Thromb Vasc Biol*. 2010; 30(12):2553–2561.
30. Lanahan AA, et al. VEGF receptor 2 endocytic trafficking regulates arterial morphogenesis. *Dev Cell*. 2010;18(5):713–724.
31. Roberts WG, Palade GE. Increased microvascular permeability and endothelial fenestration induced by vascular endothelial growth factor. *J Cell Sci*. 1995; 108(pt 6):2369–2379.
32. Nagy JA, et al. Permeability properties of tumor surrogate blood vessels induced by VEGF-A. *Lab Invest*. 2006;86(8):767–780.
33. Dejana E, Orsenigo F, Lampugnani MG. The role of adherens junctions and VE-cadherin in the control of vascular permeability. *J Cell Sci*. 2008; 121(pt 13):2115–2122.
34. Gavard J, Gutkind JS. VEGF controls endothelial-cell permeability by promoting the beta-arrestin-dependent endocytosis of VE-cadherin. *Nat Cell Biol*. 2006;8(11):1223–1234.
35. Murakami T, Felinski EA, Antonetti DA. Occludin phosphorylation and ubiquitination regulate tight junction trafficking and vascular endothelial growth factor-induced permeability. *J Biol Chem*. 2009;284(31):21036–21046.
36. Eremina V, et al. Glomerular-specific alterations of VEGF-A expression lead to distinct congenital and acquired renal diseases. *J Clin Invest*. 2003; 111(5):707–716.
37. Eremina V, et al. VEGF inhibition and renal thrombotic microangiopathy. *N Engl J Med*. 2008; 358(11):1129–1136.